

# Contrast-Enhanced MR Imaging of Lymph Nodes in Cancer Patients

Seung Hong Choi, MD  
Woo Kyung Moon, MD

## Index terms:

Magnetic resonance (MR)  
Lymph node metastasis  
Contrast media  
Magnetic resonance (MR)  
lymphography

DOI:10.3348/kjr.2010.11.4.383

## *Korean J Radiol 2010; 11: 383-394*

Received January 18, 2010; accepted after revision February 25, 2010.

All authors: Department of Radiology and the Clinical Research Institute, Seoul National University Hospital and the Institute of Radiation Medicine, Seoul National University College of Medicine, Seoul 110-744, Korea

This study was supported by a grant from the National R & D Program for Cancer Control, Ministry of Health & Welfare, Republic of Korea (A01185).

## Address reprint requests to:

Woo Kyung Moon, MD, Department of Radiology, Seoul National University College of Medicine, 101 Daehang-ro, Jongno-gu, Seoul 110-744, Korea.  
Tel. (822) 2072-3928  
Fax. (822) 743-6385  
e-mail: moonwk@radcom.snu.ac.kr

The accurate identification and characterization of lymph nodes by modern imaging modalities has important therapeutic and prognostic significance for patients with newly diagnosed cancers. The presence of nodal metastases limits the therapeutic options, and it generally indicates a worse prognosis for the patients with nodal metastases. Yet anatomic imaging (CT and MR imaging) is of limited value for depicting small metastatic deposits in normal-sized nodes, and nodal size is a poor criterion when there is no extracapsular extension or focal nodal necrosis to rely on for diagnosing nodal metastases. Thus, there is a need for functional methods that can be reliably used to identify small metastases. Contrast-enhanced MR imaging of lymph nodes is a non-invasive method for the analysis of the lymphatic system after the interstitial or intravenous administration of contrast media. Moreover, some lymphotropic contrast media have been developed and used for detecting lymph node metastases, and this detection is independent of the nodal size. This article will review the basic principles, the imaging protocols, the interpretation and the accuracies of contrast-enhanced MR imaging of lymph nodes in patients with malignancies, and we also focus on the recent issues cited in the literature. In addition, we discuss the results of several pre-clinical studies and animal studies that were conducted in our institution.

The identification of metastases in lymph nodes has a major effect on the prognosis and treatment of malignancies (1-5). Finding a single nodal metastasis can reduce a patients' prognosis by approximately one-half, regardless of the location or size of the primary tumor (2, 5). Surgical staging with lymphadenectomy and histopathologic evaluation of lymph nodes is considered the gold standard for patients with various malignancies such as prostate cancer. This technique is invasive, it is confined to the surgical field for nodal sampling (which may lead to sampling errors) and the technique has only limited accuracy (6, 7). Thus, several imaging modalities, including computed tomography (CT), magnetic resonance (MR) imaging and nuclear medicine imaging, are used to help diagnose metastatic involvement in lymph nodes (8). Yet anatomic imaging (CT and MR imaging) cannot depict small metastatic deposits in normal-sized nodes. Further, the size of nodes is a poor criterion when there is no extracapsular extension or focal nodal necrosis to rely on (9). Clinical studies have shown that enlarged lymph nodes do not necessarily contain metastases and many small nodes could be metastatic (4). Likewise, positron emission tomography (PET) with fluorine 18 fluorodeoxyglucose ( $^{18}\text{F}$ -FDG) may not depict small deposits that are below the resolution of the scanner. In addition,  $^{18}\text{F}$ -FDG is not a very selective tracer for tumor imaging since cell types other than tumor cells actively use glucose. The macrophages in inflammatory and infectious lesions can demonstrate increased  $^{18}\text{F}$ -FDG uptake, as well as the lymph nodes that are involved with granulomatous disease or

silicosis (10, 11). Thus, there is a need for functional methods that can be reliably used to identify small metastases.

There have been several recent studies that have attempted to differentiate metastases from benign lymph nodes using contrast-enhanced MR imaging of lymph nodes (LNMRI) or MR lymphography, which is a potential noninvasive method for analyzing the lymphatic system after interstitial (intracutaneous or subcutaneous) or intravenous administration of contrast media (12). Because detecting metastases depends on the contrast between benign and malignant structures, a contrast medium that accumulates either in only healthy lymphatic tissue or in only metastatic deposits may greatly increase the sensitivity and specificity of the diagnosis (13). Direct lymphatic administration has limited clinical value because the required technique is difficult and demanding, and it is also highly invasive and has associated side effects (14).

This article will review the basic principles, imaging protocols and clinical significance of contrast-enhanced LNMRI in patients with malignancies, while focusing on the recent issues cited in the literature. In addition, we also discuss the results of several pre-clinical studies and animal studies that have been done at our institution.

## The Basic Principles of Contrast-Enhanced MRI of Lymph Nodes

Interstitial administration of LNMRI contrast media (e.g., peritumoral) allows high accumulation of the contrast in regional lymph nodes. After intra- or subcutaneous injection, the compounds are taken up into the highly permeable, thin-walled, fenestrated lymphatic capillaries and they are transported with the lymph fluid to the lymph nodes. The contrast media can either target specific lymph nodal components (e.g., neoplastic cells) or be taken up by the macrophages in the nodes (8). This method can also be used for detecting sentinel lymph nodes, which are the first lymph nodes in the drainage path from a tumor site and these nodes are the location of early metastases. Identification, dissection and immunohistochemical evaluation of these sentinel nodes could be sufficient for tumor N-staging (nodal metastases) (13). This mode of contrast media administration seems to be the most feasible for breast cancers, melanomas, head and neck cancers and rectal cancers. Interstitial contrast-enhanced LNMRI can be performed with several types of contrast media, including extracellular contrast media, extracellular contrast media encapsulated in liposomes, superparamagnetic iron oxide particles, polymeric compounds and lipophilic compounds that form aggregates or micelles (15–24). The potential problems of the interstitial route of contrast media

**Table 1. Contrast Medias Reported in Literature for Contrast-Enhanced LNMRI**

	Generic Name	Trade Name	Injection Route	Lymph Node Specificity	Compound Type	Human Application	References
Gadolinium-based contrast media	Gadopentetate dimeglumine	Magnevist	Interstitial	No	Chelate	Yes	29
	Gadoterate meglumine	Dotarem	Interstitial	No	Chelate	Yes	30
	Gadodiamide	Omniscan	Interstitial	No	Chelate	Yes	16
	Gadobutrol	Gadovist	Interstitial	No	Liposome encapsulated	Yes	17, 31
	Gadopentetate dimeglumine-PE	-	Interstitial	No	Liposome encapsulated	No	32
	Gadopentetate dimeglumine-PGM	-	Interstitial/intravenous	Yes	Polymer	No	19, 33
	PAMAM dendrimer based medium	-	Interstitial	No	Polymer	No	34, 35
	SHL643A	Gadomer-17	Interstitial	No	Polymer	No	36
	NC22181, NC66386	-	Interstitial	No	Polymer	No	37
	Gadomelitol	Vistarem	Interstitial	No	Polymer	Yes	38
	Gadofosveset trisodium	Vasovist	Interstitial	No	Albumin binding	Yes	39
	Gadofluorine 8	-	Interstitial	Yes	Micelle	No	21, 22
Gadofluorine M	-	Interstitial/intravenous	Yes	Micelle	No	12, 40, 41	
Iron oxide-based contrast media	Ferumoxide	Feridex/Endorem	Interstitial	No	SPIO	Yes	23
	Ferumoxtran-10	Combidx/Sinerem	Interstitial/intravenous	Yes	USPIO	Yes	24, 42
	MION-46, 47	-	Interstitial/intravenous	Yes	USPIO	No	27, 43

Note. — LNMRI = MRI of lymph nodes, MION = monocrystalline iron oxide nanoparticle, PAMAM = polyamidoamine, PE = phosphatidylethanolamine, PGM = polyglucose associated macrocomplex, SPIO = superparamagnetic iron oxide, USPIO = ultrasmall superparamagnetic iron oxide

administration include evaluation of lymph nodes that are distal to a lymphatic obstruction and that are not opacified, and evaluation of lymph nodes on the contralateral side, which would necessitate multiple injections (25, 26).

Intravenous contrast-enhanced LNMRI offers a noninvasive means of potentially analyzing the lymphatic system (12). Intravenous injection of a lymphotropic contrast medium is preferable to interstitial administration because the intravenously injected contrast medium is distributed to each individual lymph node (12). Intravenously administered contrast media for LNMRI tends to accumulate in the organs belonging to the reticuloendothelial system. The ideal LNMRI contrast medium would accumulate in all lymph nodes after intravenous injection, making it useful for lymph node staging for all types of cancer. In contrast to an interstitial application, intravenous injection is investigator independent and it may result in a more reproducible imaging. In tumor-bearing lymph nodes, the functional lymph node tissue and sinusoidal macrophages are replaced by tumor cells (27). Contrast medium will be taken up by the functional lymph node tissue, but not by the tumor cells, resulting in high signal contrast between the benign and malignant structures (13).

Although the exact mechanism for the transfer of intravenously injected contrast media into the lymphatic tissue is largely unknown, two main pathways are possible. The first mechanism is a nonspecific capillary extravasation through transendothelial channels into the interstitial space and the subsequent uptake into primary lymphatic vessels, followed by transport to the lymph nodes (28). This route appears to be responsible for the delayed accumulation of iron oxide particles and a dextran-conjugated gadopente-

tate dimeglumine-polyglucose associated macrocomplex (PGM). The second pathway is direct transcappillary passage through the interendothelial junctions into the medullary sinuses within the lymph nodes (28). This is probably the main mechanism for the rapid lymph node uptake of gadofluorine M (Bayer Schering Pharma, Germany), and it might also play a role in the uptake of dextran-coated particles.

Intravenous administration may have some drawbacks: (i) the heterogeneous distribution between different groups of lymph nodes in the body, (ii) the high requirements regarding systemic tolerance of the contrast medium, (iii) the requirement for a higher dose, (iv) it has no potential to detect the sentinel lymph nodes and (v) there is no visualization of lymphatic vessels. The intravenous injection mode is preferable for lung cancers, colon cancers, head and neck cancers, testicular carcinomas, cervical and ovarian cancers and lymphomas (13).

Table 1 summarizes the contrast medias that have been reported on in the literature for contrast-enhanced LNMRI (12, 16, 17, 19, 21–24, 27, 29–43).

### Ultrasmall Superparamagnetic Iron Oxide (USPIO)-Enhanced MRI of Lymph Nodes

Ferumoxtran-10 (Combidex [Advanced Magnetics, Cambridge, MA]; also known as Sinerem, AMI-7227, AMI-227 and BMS 180549) is a reticuloendothelial system-targeted MR imaging contrast medium that consists of USPIO particles, and this was specifically developed for contrast-enhanced LNMRI and to improve the detection of minimal nodal metastases (28, 44–47). Even though the

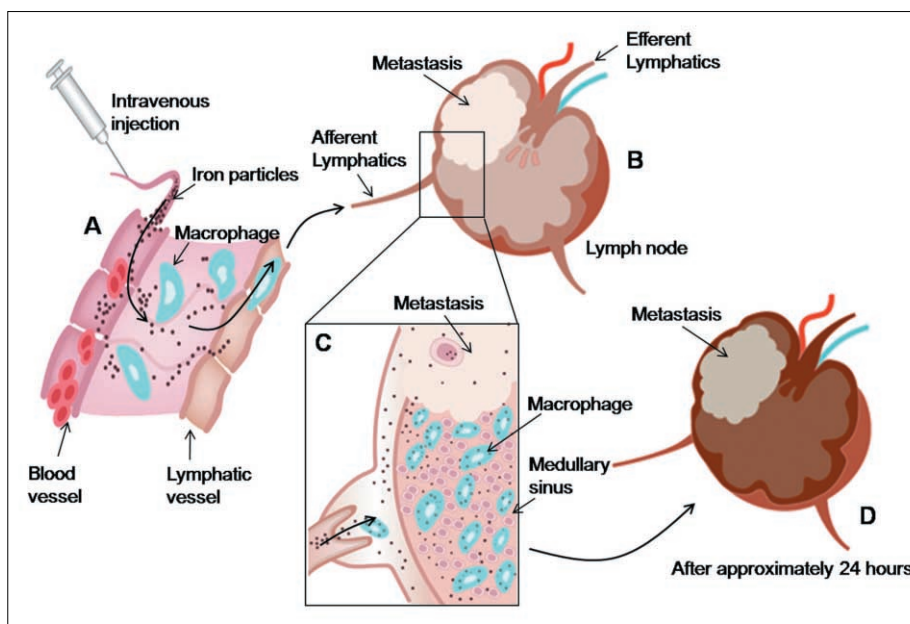


**Fig. 1.** Uptake mechanism of ferumoxtran-10. **A.** Intravenously injected particles slowly extravasate from vascular space to interstitial space. **B.** Particles are then transported to lymph nodes via lymphatic vessels. **C.** In lymph nodes, particles are internalized by macrophages. **D.** These intracellular iron-containing particles cause normal nodal tissue to have low signal intensity. Disturbances of lymph flow or nodal architecture by metastases lead to abnormal accumulation patterns, as is depicted by lack of decreased signal intensity.

cost of ferumoxtran-10 is higher than the other commercially available MRI contrast medias, there have been several promising reports for the detection of lymph node metastasis by using ferumoxtran-10-enhanced LNMRI. These USPIO nanoparticles are composed of an iron oxide crystalline core of 4.3–6.0 nm covered by low-molecular-weight dextran. The T1 and T2 relaxivities of these nanoparticles in 0.5% agar are  $2.3 \times 10^4$  and  $5.3 \times 10^4$  mol<sup>-1</sup> sec<sup>-1</sup> (20 MHz, 39°C), respectively (48).

After intravenous injection of the recommended dose of 2.6 mg of iron per kilogram of body weight, the ferumoxtran-10 particles are transported into the interstitial space and subsequently into the lymph nodes via the lymph vessels (48). Once within the normally functioning nodes, the iron particles are phagocytosed by the macrophages, and this reduces the signal intensity of the normal lymph nodes in which they accumulate due to the susceptibility effects of iron oxide reducing T2\*. Macrophage activity is absent in the areas of lymph nodes that are replaced by malignant cells, and so there is a lack of ferumoxtran-10 uptake (Fig. 1). Thus, post-ferumoxtran-10 MRI allows identification of metastatic areas within the lymph nodes and this is independent of the lymph node size (49).

Ferumoxtran-10 is well-tolerated and it has a favorable safety profile (50). However, ferumoxtran-10 is contraindicated for patients with known hypersensitivity or anaphylactic reaction to ferumoxtran-10 or any component of the product. Thus, physicians should make an effort to prevent such reactions. Due to the observed maternotoxic and teratogenic effects of ferumoxtran-10 in animals, ferumoxtran-10 is contraindicated in women of child-bearing potential and who are not using effective contraception,

and during pregnancy and breastfeeding (51). Medical supervision for 60 minutes from the start of the infusion is required because of the potential for severe allergic, anaphylactic or infusion-like reactions. Patients with a history of hypersensitivity, including allergy to an iodinated contrast medium, should be carefully monitored as the risk of adverse reactions, and particularly allergic reactions, is increased. The most common adverse event reported in the studies that were evaluated in a metaanalysis was mild lumbar back pain and this occurred in fewer than 4% of patients (52). Other adverse effects were headache, vasodilatation and urticaria. None of the adverse events were serious, with most being mild or moderate in severity and of a short duration.

**Imaging Technique**

It has been standard practice to perform lymphotropic nanoparticle imaging with two MRI scans at about 24–36 hours apart (42, 53). This time lag before performing the post-contrast imaging is essential to allow sufficient extraction of the ferumoxtran-10 by the normal functioning macrophages within the nodes. If the imaging is performed prematurely, then the lack of sufficient nodal uptake within benign nodes may lead to their erroneous characterization as malignant nodes (49).

The precontrast imaging is primarily used for staging the primary tumor. The T1-weighted gradient recalled echo (GRE) and T2-weighted fast spin-echo sequences are used for anatomic localization; the T1-weighted sequence in particular is necessary for identification of a fatty hilum. Such identification is critical for correct interpretation of the postcontrast images. A T2\*-weighted GRE sequence is

Benign Lymph Nodes			Metastatic Lymph Nodes		
Pre-USPIO T2*WI	Post-USPIO T2*WI	Description	Pre-USPIO T2*WI	Post-USPIO T2*WI	Description
		Node has overall dark signal intensity			No blackening of node. Node is hyperintense to surrounding tissue
		Node has overall dark signal apart from the fatty hilum			Node has eccentric high signal with darkening along the peripheral rim
		Node has central low signal intensity			Node has central high signal with darkening along the peripheral rim
		Node has central low signal intensity			
		Node has an overall dark signal with tiny areas of high signal within it			

**Fig. 2.** Patterns of ultrasmall superparamagnetic iron oxide (USPIO) uptake in benign and malignant lymph nodes on contrast-enhanced MRI of Lymph nodes, and respective interpretations of these patterns.

## Enhanced MR Imaging of Malignant Lymph Nodes

then performed. Although USPIO shortens the T1 and T2\* relaxation times, it is the T2\*-weighted sequence that is most sensitive to the susceptibility changes induced by the intranodal nanoparticles. In addition, the T2\*-weighted sequences are superior for nodal characterization on the postcontrast images as compared to that of the fast spin-echo T2-weighted sequences (54). Therefore, the imaging parameters should be optimized to enhance the T2\* weighting while minimizing the T1 effects (54, 55). The T2\*-weighted sequence should ideally be a heavily T2\*-weighted GRE acquisition with a long echo time and a small flip angle, since a short echo time may lead to an inadequate signal drop (49).

Some investigators have recently reported modified imaging protocols to improve the accuracy of detecting malignant lymph nodes and to save the scan time without decreasing the diagnostic accuracy. Acquiring a dual echo time (TE) T2\*-weighted sequence with intermediate and long TE values improves nodal characterization. Saksena et al. (54) showed that images with a TE of 21 msec showed higher specificity, but low sensitivity, whereas the images with a TE of 12.2 msec showed higher sensitivity, but lower specificity. This was attributed to the longer TE detecting even small concentrations of ferumoxtran-10 within nodes, and so more true-negative nodes are identified. Saksena et al. (54) found that there is no significant

difference in the diagnostic precision between paired MRI (unenhanced MRI followed by ferumoxtran-10 enhanced MRI) and post-contrast MRI alone for an experienced reviewer. The heavily T1-weighted images remain unaffected by ferumoxtran-10. These images could also be obtained after administration of ferumoxtran-10 and they do not require a separate unenhanced imaging session. The high-resolution LNMRI technique also showed promising results of 100% accuracy to differentiate benign and malignant lymph nodes; Kimura et al. (56) performed high resolution ferumoxtran-10-enhanced LNMRI with a section thickness of 3 mm, a  $256 \times 256$  matrix and a small field of view ( $10 \times 10 - 16 \times 16$  cm) using a 3-inch surface coil in breast cancer patients, and they evaluated sentinel lymph nodes. However, this technique is limited to evaluating distant lymph nodes.

Clinical 3.0T whole-body MRI systems are becoming increasingly available. Heesackers et al. (57) reported that ferumoxtran-10 enhanced MRI at 3.0T improved the image quality as compared with 1.5T MRI, and the former has the possibility of increased detection of small metastatic lymph nodes. However, we found that 3.0T monocrystalline iron oxide nanoparticle (MION)-47 enhanced MRI had a higher specificity as compared to that of 1.5T imaging without a significant difference of sensitivity in a rabbit VX2 model (58). It was mainly because of the T2\*

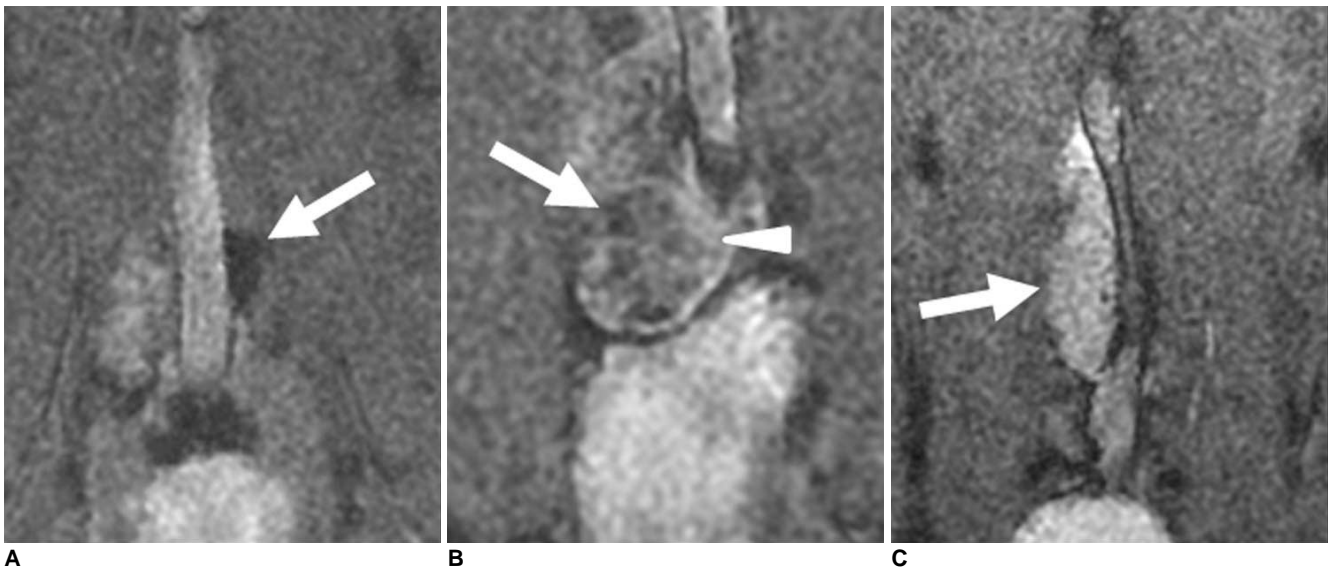


**Fig. 3.** Benign and metastatic lymph nodes on ultrasmall superparamagnetic iron oxide (MION [monocrystalline iron oxide nanoparticle]-47)-enhanced MR imaging in three rabbit VX2 tumor models.

**A.** T2\*-weighted MR image obtained 24 hours after intravenous administration of MION-47 (2.6 mg of iron per kilogram of body weight) shows homogeneous dark signal intensity of benign left paraaortic lymph node (arrow).

**B.** T2\*-weighted MR image obtained 24 hours after intravenous administration of MION-47 (2.6 mg of iron per kilogram of body weight) shows focal high signal intensity region (arrowhead) in right paraaortic lymph node (arrow), which was proven to be metastatic focus by histopathology.

**C.** T2\*-weighted MR image obtained 24 hours after intravenous administration of MION-47 (2.6 mg of iron per kilogram of body weight) shows malignant right paraaortic lymph node (arrow), which was totally replaced with metastatic tissue.

susceptibility artifact that appears to shadow the small metastasis in lymph nodes.

### Image Interpretation

On the pre-contrast T2\*-weighted images, both the benign and malignant nodes appear bright. After USPIO administration, the benign nodes are typically black on the T2\*-weighted images and the malignant nodes remain bright on the post-contrast T2\*-weighted images. However, there is a spectrum of appearances between these two extremes (55). These patterns of USPIO uptake and their interpretations are given in Figure 2 (53, 55), which are based on the qualitative analysis of the readers.

Lahaye et al. (59) reported that an estimated area of the white region within the node that was larger than 30% was highly predictive for discriminating between benign and malignant lymph nodes, with a sensitivity of 93% and a specificity of 96%. They measured the percentage of white lesions (high signal intensity) within the lymph node. A high signal intensity or white region in lymph nodes is caused by no or very little uptake of USPIO in that part of the lymph nodes. Our study shows that the larger the area of the white region, the more likely that the node is malignant (Fig. 3).

Some pitfalls in the interpretation of USPIO-enhanced LNMRI have been reported. First, the normal fatty hilum of a node can mimic a central metastatic deposit because it shows bright signal intensity on both the pre- and post-contrast T2\*-weighted images. The T1-weighted sequence will help reduce this misinterpretation by allowing correct characterization of the fat within the nodal hilum (55). Second, reactive hyperplasia of lymph nodes is known to be one of the reasons for false positives. The lymphoid

follicles, which are located in the cortex, have few macrophages and the lymphoid follicles appear as relatively high signal intensity compared with the signal intensity of the medulla (60). When lymph nodes undergo reactive enlargement, there is frequently cortical or paracortical hyperplasia, which results in an increase in the size of the lymphoid follicles and the node's cortical thickness. Since the macrophages predominantly remain within the medullary sinus, the susceptibility effects of USPIO in a reactive lymph node can appear confined to the center of the node, and this appearance gives rise to the pattern of central low signal intensity (61). Third, granulomatous disease can cause necrosis within lymph nodes, resulting in areas within the lymph node that are devoid of macrophages. This appearance may be indistinguishable from that of a metastatic node on the postcontrast T2\*-weighted images (55). Nodal fibrosis can cause a similar appearance, as was observed in a study by Saksena et al. (54). Fourth, the relatively poor contrast between the metastasis and the surrounding extralymphatic tissue on the T2\*-weighted images makes the detection of subcapsular metastases difficult, and it has also been suggested that micrometastases in the germinal center may not be seen due to the scarcity of macrophages in this area (40, 60, 62).

### Diagnostic Accuracy

Despite these limitations, the reported accuracy of this novel technique supersedes the conventional parameters described earlier. Harisinghani et al. (42) reported a sensitivity of 100% with a specificity of 96% for characterizing lymph nodes in patients with prostate cancer. Of note, 71% of the histopathologically proven malignant

**Table 2. Summary of Published Clinical Trials with Ultrasmall Superparamagnetic Iron Oxide**

References			No. of Patients	Region	USPIO-Enhanced MRI*		
Authors	No.	Year			Sensitivity (%)	Specificity (%)	Accuracy (%)
Anzai et al.	63	1994	11	Head and neck	95	84	-
Bellin et al.	64	1998	30	Pelvis retroperitoneum	100	80	-
Sigal et al.	65	2002	81	Head and neck	88	77	-
Stets et al.	66	2002	9	Breast	81	92	87
Mack et al.	67	2002	30	Head and neck	86	100	-
Anzai et al.	53	2003	147	All body regions	83	77	80
Harisinghani et al.	42	2003	80	Pelvis	91	96	-
Deserno et al.	68	2004	58	Pelvis	96	98	-
Rockall et al.	69	2005	44	Pelvis	91-100	87-94	-
Stadnik et al.	70	2006	10	Breast	100	80	-
Saksena et al.	54	2006	65	All body regions	87	96	-
Memarsadeghi et al.	71	2006	22	Breast	100	98	98
Lahaye et al.	59	2008	28	Pelvis	93	96	-
Heesakkers et al.	72	2008	375	Pelvis	82	93	-

Note. — \* Data are based on node-by-node assessment. USPIO = ultrasmall superparamagnetic iron oxide

Enhanced MR Imaging of Malignant Lymph Nodes

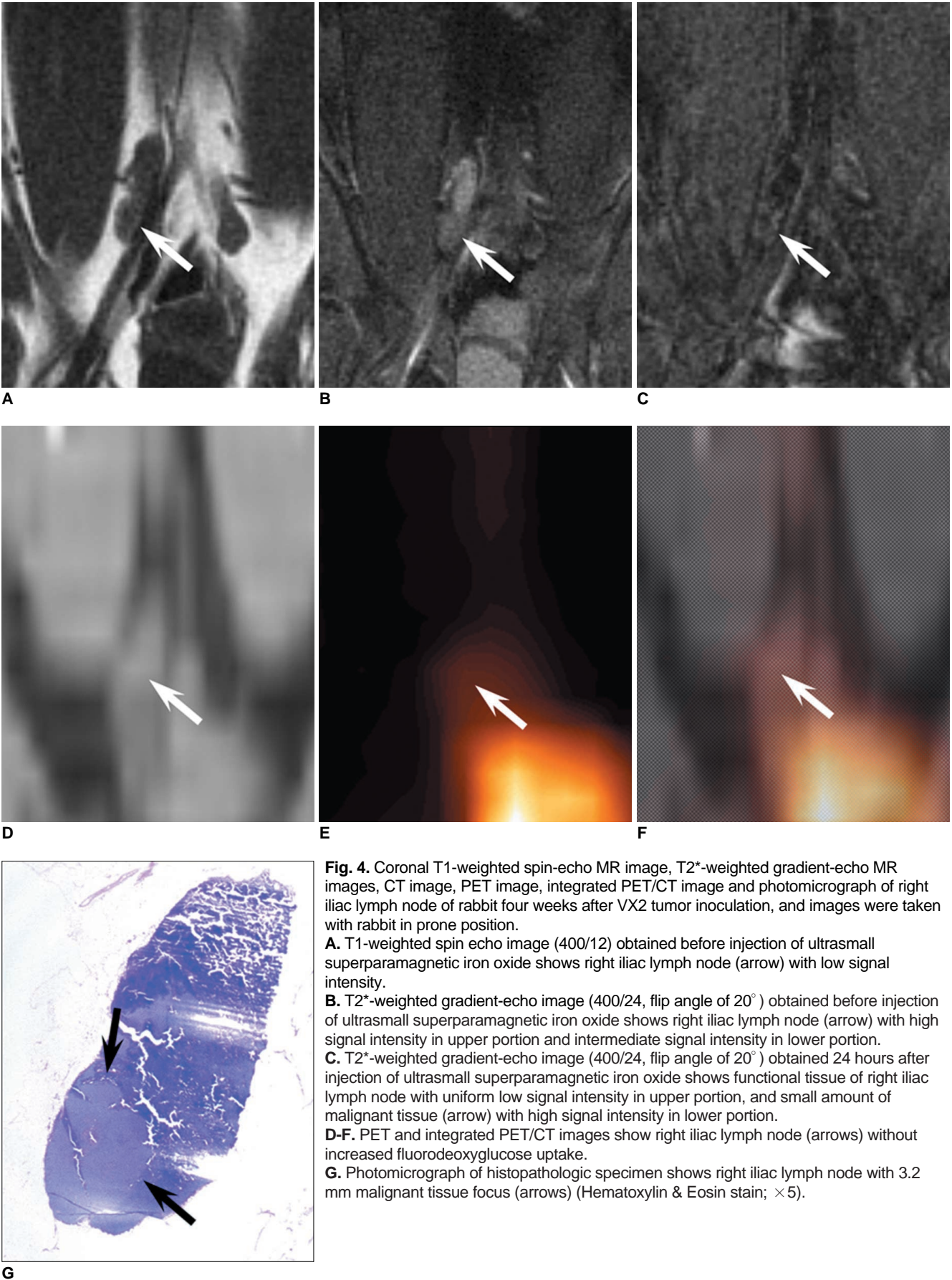


**Fig. 4.** Coronal T1-weighted spin-echo MR image, T2\*-weighted gradient-echo MR images, CT image, PET image, integrated PET/CT image and photomicrograph of right iliac lymph node of rabbit four weeks after VX2 tumor inoculation, and images were taken with rabbit in prone position.  
**A.** T1-weighted spin echo image (400/12) obtained before injection of ultrasmall superparamagnetic iron oxide shows right iliac lymph node (arrow) with low signal intensity.  
**B.** T2\*-weighted gradient-echo image (400/24, flip angle of 20°) obtained before injection of ultrasmall superparamagnetic iron oxide shows right iliac lymph node (arrow) with high signal intensity in upper portion and intermediate signal intensity in lower portion.  
**C.** T2\*-weighted gradient-echo image (400/24, flip angle of 20°) obtained 24 hours after injection of ultrasmall superparamagnetic iron oxide shows functional tissue of right iliac lymph node with uniform low signal intensity in upper portion, and small amount of malignant tissue (arrow) with high signal intensity in lower portion.  
**D-F.** PET and integrated PET/CT images show right iliac lymph node (arrows) without increased fluorodeoxyglucose uptake.  
**G.** Photomicrograph of histopathologic specimen shows right iliac lymph node with 3.2 mm malignant tissue focus (arrows) (Hematoxylin & Eosin stain; × 5).

nodes did not fulfill the traditional imaging criteria for malignancy. Anzai et al. (53), when reporting on an overall phase III multicenter trial for evaluating various primary cancers, reported a sensitivity, specificity and accuracy of 85%, 85% and 85%, respectively, with using the post-contrast imaging alone and 83%, 77% and 80%, respectively, with the paired pre- and post-contrast MRI. In a recent meta-analysis, 19 prospective studies that compared MRI, with or without ferumoxtran-10 enhancement, with the histopathological diagnosis were used for data analysis and extraction. The authors showed that ferumoxtran-10-enhanced MRI has a higher diagnostic accuracy than unenhanced MRI for diagnosing lymph node metastases. The summary receiver operating characteristic (ROC) curve analysis for the per-lymph-node data showed an overall sensitivity of 88% and an overall specificity of 96% for ferumoxtran-10-enhanced MRI (52). A summary of the various reported series on ferumoxtran-10-enhanced MRI is shown in Table 2 (42, 53, 54, 59, 63-72).

Ultrasmall superparamagnetic iron oxide-enhanced MRI and PET/CT are current known to be the most advanced imaging tools to improve the accuracy of nodal staging in a non-invasive manner. There has been no clinical data concerning direct comparison of USPIO-enhanced MRI versus PET/CT for the detection of lymph node metastasis. Stadnik et al. (70) reported that USPIO-enhanced MR imaging for the axillary lymph node staging in breast cancer patients showed a sensitivity of 100% and a specificity of 80%, while a sensitivity of 80% and a specificity of 100% were achieved for  $^{18}\text{F}$ -FDG PET. However, our experimental study using a rabbit VX2 carcinoma model showed MION-47-enhanced MRI had a higher sensitivity (86%, 6 of 7) than PET/CT (0%, 0 of 7) for detecting small (< 5 mm) metastases (43) (Fig. 4).

### Gadolinium-Enhanced MRI of Lymph Nodes

Gadolinium-based compounds seem to have a potential for the future clinical application of LNMRI. Gadolinium-enhanced MR images exhibit higher spatial resolution, a higher signal-to-noise ratio and fewer artifacts than do the MR images enhanced with T2\* media such as iron oxide particles (19, 44). However, the major drawback of gadolinium-based contrast media for LNMRI is that there has been no clinically available lymphotropic gadolinium media. Thus, in this session of the paper, we reviewed a few clinical trials that used interstitial contrast-enhanced LNMRI with gadolinium chelates or blood pool media, and other experimental studies for the future clinical application of interstitial or intravenous contrast-enhanced LNMRI with modified gadolinium media (Table 1).

### Interstitial Contrast-Enhanced MRI of Lymph Nodes

Interstitial contrast-enhanced LNMRI with the commercially available extracellular gadolinium chelates such as gadopentetate dimeglumine, gadoterate meglumine and gadodiamide have been performed in humans. Interstitial contrast-enhanced LNMRI with gadopentetate dimeglumine is a feasible modality for breast sentinel lymph node mapping, and so it can be used for performing surgical biopsy of the breast sentinel lymph node (29). Ruehm et al. (30) evaluated the lymphatic system of the lower extremities on interstitial contrast-enhanced LNMRI with gadoterate meglumine, which allowed visualization of the draining lymph vessels and nodes; in one patient, an inguinal fluid collection could be characterized as a lymphocele, and a chylothorax was diagnosed in one infant. However, these techniques are limited by their inability to differentiate between benign and malignant lymph nodes in cancer patients.

Several modified gadolinium contrast medias have been developed, and interstitial contrast-enhanced LNMRI with using some of these contrast medias has been investigated for the detection of malignant lymph nodes in tumor-bearing animal models. The newly developed gadolinium media can provide higher T1-relaxivity than that of the

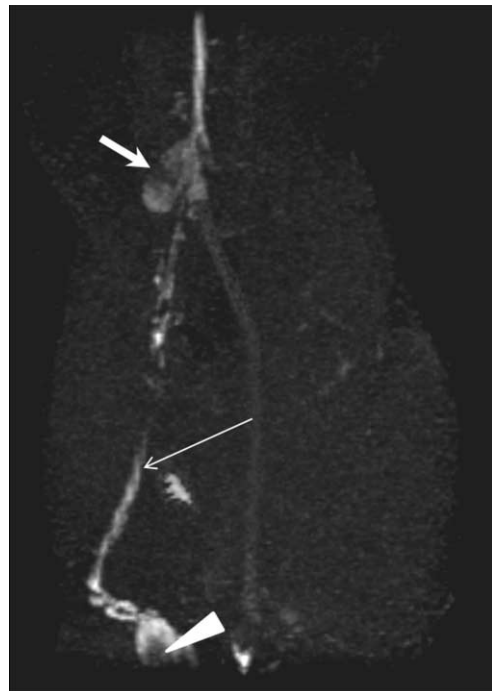


**Fig. 5.** Oblique coronal maximum intensity projection image from T1-weighted 3D gradient-echo MRI sequence obtained 60 minutes after interstitial administration of 5  $\mu\text{mol}/\text{kg}$  gadofluorine M in VX2 tumor rabbit model. Metastases in right popliteal (arrowhead) and iliac (thick arrow) lymph nodes are demonstrated as filling defects. Lymphatic vessels (thin arrow) are also sharply delineated.

## Enhanced MR Imaging of Malignant Lymph Nodes

conventional extravascular contrast media; the materials include liposome-encapsulated media (gadobutrol and gadopentetate dimeglumine-PE), polymeric media (gadopentetate dimeglumine-PGM, PAMAM dendrimer based medium, SHL643A, NC22181, NC66386 and gadomelitol), protein-binding compounds (gadofosveset trisodium) or micelle-forming media (gadofluorine 8 and M) (12, 21, 31, 32, 34–39, 41). These media enabled the visualization of the lymphatic system and the detection of

lymph node metastases, which were demonstrated as filling defects in the lymph nodes (Fig. 5). Among those medias, gadobutrol, gadomelitol and gadofosveset trisodium can be used for human application as a blood pool medium.

### *Intravenous Contrast-Enhanced MRI of Lymph Nodes*

The intravenous injection of conventional extracellular contrast media (gadopentetate dimeglumine) could improve the identification and characterization of the

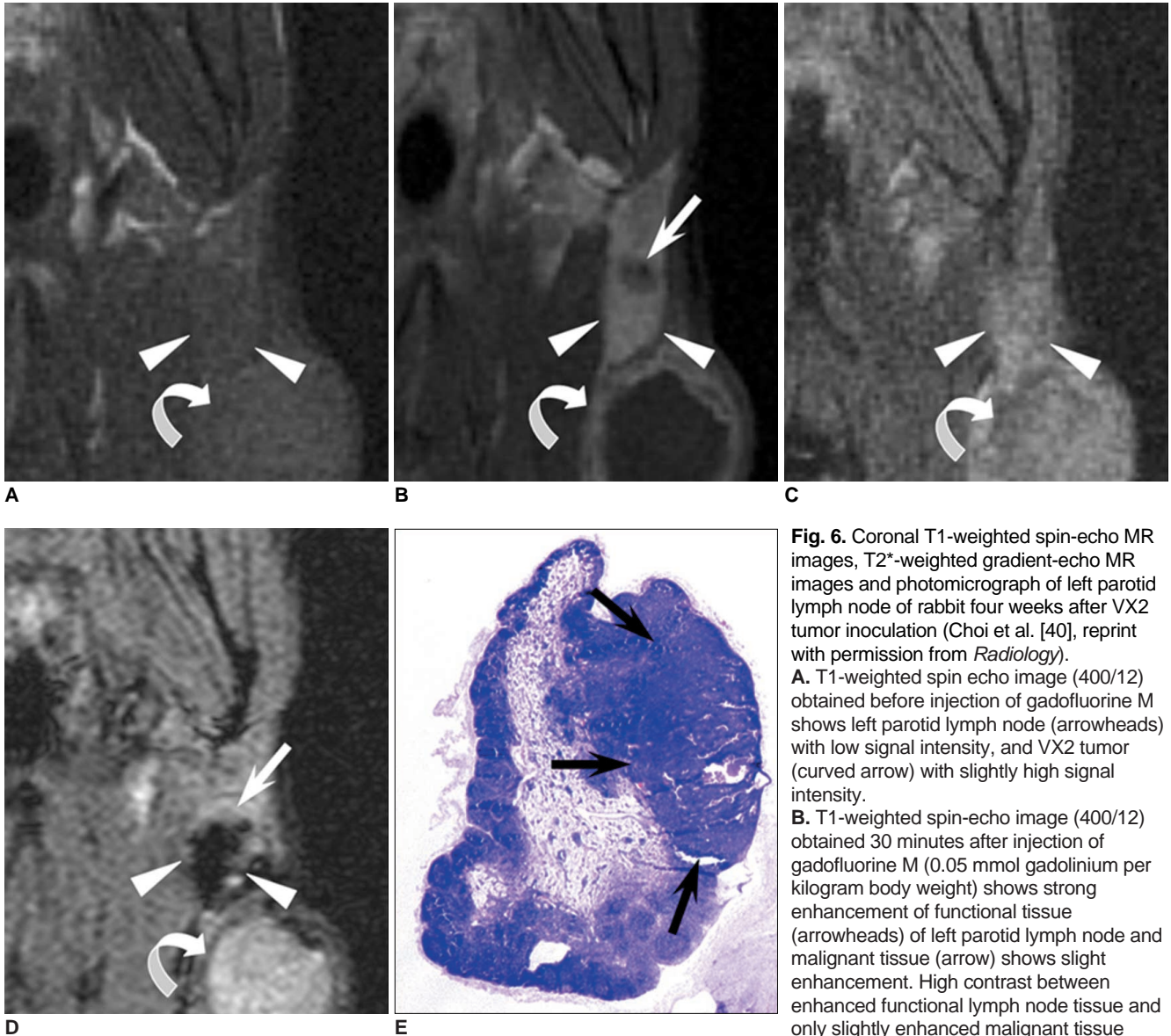


**Fig. 6.** Coronal T1-weighted spin-echo MR images, T2\*-weighted gradient-echo MR images and photomicrograph of left parotid lymph node of rabbit four weeks after VX2 tumor inoculation (Choi et al. [40], reprint with permission from *Radiology*).  
**A.** T1-weighted spin-echo image (400/12) obtained before injection of gadofluorine M shows left parotid lymph node (arrowheads) with low signal intensity, and VX2 tumor (curved arrow) with slightly high signal intensity.  
**B.** T1-weighted spin-echo image (400/12) obtained 30 minutes after injection of gadofluorine M (0.05 mmol gadolinium per kilogram body weight) shows strong enhancement of functional tissue (arrowheads) of left parotid lymph node and malignant tissue (arrow) shows slight enhancement. High contrast between enhanced functional lymph node tissue and only slightly enhanced malignant tissue  
**C.** T2\*-weighted gradient-echo image (400/24, flip angle of 20°) obtained before injection of MION-47 shows left parotid lymph node (arrowheads) with high signal intensity, and VX2 tumor (curved arrow) with high signal intensity.  
**D.** T2\*-weighted gradient-echo image (400/24, flip angle of 20°) obtained 24 hours after injection of MION-47 (2.6 mg of iron per kilogram of body weight) shows functional tissue (arrowheads) of left parotid lymph node with uniform low signal intensity and peripheral malignant tissue (arrow) with high signal intensity, which shows poor contrast between malignant tissue and surrounding parenchymal tissue. High signal intense VX2 tumor (curved arrow) with peripheral low signal intensity is also noted.  
**E.** Photomicrograph of histopathologic specimen shows malignant tissue (arrows) with maximum diameter of 2 mm in subcapsular portion of left parotid lymph node (Hematoxylin & Eosin stain; original magnification, ×5).

enables more obvious detection of metastasis than in (D). VX2 tumor (curved arrow) with peripheral rim enhancement is also noted.

lymph nodes (the enhancement characteristics and the size, shape and contour). The enhancement pattern of malignant lymph nodes is histologically-related to nodal necrosis. A significantly longer time to peak, a lower peak enhancement, a lower maximum slope and a lower washout slope were found in tumor-involved lymph nodes as compared with that of normal lymph nodes (73, 74). However, these compounds have no specific accumulation in the nodes and they do not clearly differentiate between functional and metastatic lymph node tissue (75, 76).

The first lymphotropic gadolinium-based contrast was gadopentetate dimeglumine-PGM, which was administered intravenously and it showed accumulation in the physiologic lymphatic tissue in a rat model (33). A water-soluble, macrocyclic, gadolinium-based T1-contrast medium (gadofluorine M) was recently reported to accumulate in functional lymph node tissue after intravenous injection (12). The compound contains a perfluorinated side chain that is responsible for the formation of micelles in aqueous solutions and for hydrophobic protein interaction. MRI of VX2 tumor-bearing rabbits revealed a rapid, dose-dependent signal increase in the functional lymph node tissue starting within 5 min post-injection and it reached a maximum at 60–90 min. The contrast medium enabled detecting lymph node metastases that were greater than 1 mm in an animal model. The effects are related to both the blood pool effect of the contrast medium and to an additional subsequent accumulation in the functional lymph node tissue (12). In terms of contrast-enhanced LNMRI, gadofluorine M has the following two benefits compared with USPIO particles: 1) a complete pre- and post-contrast MR imaging examination is performed in one session and 2) the high contrast between malignant and functional lymph node tissues facilitates the detection of lymph node metastases. Interestingly, our experimental study showed that gadofluorine M-enhanced MR imaging has higher accuracy for depicting lymph node metastases than does USPIO (MION-47)-enhanced MR imaging in a rabbit VX tumor model (40) (Fig. 6).

## CONCLUSION

Differentiation between malignant and benign lymph nodes on oncologic imaging is of major interest when determining the therapeutic plan. There is currently no accepted ideal imaging modality or technique for diagnosing lymph node metastases. Contrast-enhanced LNMRI seems to be a promising noninvasive modality for evaluating lymph nodes in patients with malignancies. This technique may allow functional and anatomic definition in one investigation. However, the contrast-enhanced LNMRI

techniques with contrast media need to be evaluated for their future clinical applications, as none of the above-mentioned lymphotropic contrast medias are currently approved for use in humans for contrast-enhanced LNMRI. Only ferumoxtran-10 has reached the stage of clinical trials for this indication. Another drawback of contrast-enhanced LNMRI is that it cannot detect micrometastases of less than 1 mm in lymph nodes (25). Further development of MR imaging techniques such as increased field strength, better coils and optimized sequences will improve detecting micrometastases in the future.

## Acknowledgment

We thank Yoon Kyeong Choi for the illustration.

## References

- King AD, Tse GM, Ahuja AT, Yuen EH, Vlantis AC, To EW, et al. Necrosis in metastatic neck nodes: diagnostic accuracy of CT, MR imaging, and US. *Radiology* 2004;230:720-726
- Anzai Y, Brunberg JA, Lufkin RB. Imaging of nodal metastases in the head and neck. *J Magn Reson Imaging* 1997;7:774-783
- Gershenwald JE, Thompson W, Mansfield PF, Lee JE, Colome MI, Tseng CH, et al. Multi-institutional melanoma lymphatic mapping experience: the prognostic value of sentinel lymph node status in 612 stage I or II melanoma patients. *J Clin Oncol* 1999;17:976-983
- Laiyy JP, Gay-Depassier P, Soyer P, Dombret MC, Murciano G, Sautet A, et al. Enlarged mediastinal lymph nodes in bronchogenic carcinoma: assessment with dynamic contrast-enhanced MR imaging. Work in progress. *Radiology* 1994;191:263-267
- van den Brekel MW. Lymph node metastases: CT and MRI. *Eur J Radiol* 2000;33:230-238
- Davis GL. Sensitivity of frozen section examination of pelvic lymph nodes for metastatic prostate carcinoma. *Cancer* 1995;76:661-668
- Torabi M, Aquino SL, Harisinghani MG. Current concepts in lymph node imaging. *J Nucl Med* 2004;45:1509-1518
- Moghimi SM, Bonnemain B. Subcutaneous and intravenous delivery of diagnostic agents to the lymphatic system: applications in lymphoscintigraphy and indirect lymphography. *Adv Drug Deliv Rev* 1999;37:295-312
- Puri SK, Fan CY, Hanna E. Significance of extracapsular lymph node metastases in patients with head and neck squamous cell carcinoma. *Curr Opin Otolaryngol Head Neck Surg* 2003;11:119-123
- Kapucu LO, Meltzer CC, Townsend DW, Keenan RJ, Luketich JD. Fluorine-18-fluorodeoxyglucose uptake in pneumonia. *J Nucl Med* 1998;39:1267-1269
- Rennen HJ, Corstens FH, Oyen WJ, Boerman OC. New concepts in infection/inflammation imaging. *Q J Nucl Med* 2001;45:167-173
- Misselwitz B, Platzek J, Weinmann HJ. Early MR lymphography with gadofluorine M in rabbits. *Radiology* 2004;231:682-688
- Misselwitz B. MR contrast agents in lymph node imaging. *Eur J Radiol* 2006;58:375-382
- Witte CL, Williams WH, Witte MH. Lymphatic imaging. *Lymphology* 1993;26:109-111

## Enhanced MR Imaging of Malignant Lymph Nodes

15. Ruehm SG, Corot C, Debatin JF. Interstitial MR lymphography with a conventional extracellular gadolinium-based agent: assessment in rabbits. *Radiology* 2001;218:664-669
16. Lohrmann C, Földi E, Bartholomä JP, Langer M. MR imaging of the lymphatic system: distribution and contrast enhancement of gadodiamide after intradermal injection. *Lymphology* 2006;39:156-163
17. Misselwitz B, Sachse A. Interstitial MR lymphography using Gd-carrying liposomes. *Acta Radiol Suppl* 1997;412:51-55
18. Weissleder R, Elizondo G, Josephson L, Compton CC, Fretz CJ, Stark DD, et al. Experimental lymph node metastases: enhanced detection with MR lymphography. *Radiology* 1989;171:835-839
19. Harika L, Weissleder R, Poss K, Zimmer C, Papisov MI, Brady TJ. MR lymphography with a lymphotropic T1-type MR contrast agent: Gd-DTPA-PGM. *Magn Reson Med* 1995;33:88-92
20. Staatz G, Nolte-Ernsting CC, Bücker A, Misselwitz B, Grosskortenhau S, Pflüger D, et al. Interstitial T1-weighted MR lymphography with use of the dendritic contrast agent Gadomer-17 in pigs. *Rofo* 2001;173:1131-1136
21. Misselwitz B, Platzek J, Radiüchel B, Oellinger JJ, Weinmann HJ. Gadofluorine 8: initial experience with a new contrast medium for interstitial MR lymphography. *MAGMA* 1999;8:190-195
22. Staatz G, Nolte-Ernsting CC, Adam GB, Grosskortenhau S, Misselwitz B, Bücker A, et al. Interstitial T1-weighted MR lymphography: lipophilic perfluorinated gadolinium chelates in pigs. *Radiology* 2001;220:129-134
23. Motoyama S, Ishiyama K, Maruyama K, Okuyama M, Sato Y, Hayashi K, et al. Preoperative mapping of lymphatic drainage from the tumor using ferumoxide-enhanced magnetic resonance imaging in clinical submucosal thoracic squamous cell esophageal cancer. *Surgery* 2007;141:736-747
24. Bengele HH, Palmacci S, Rogers J, Jung CW, Crenshaw J, Josephson L. Biodistribution of an ultrasmall superparamagnetic iron oxide colloid, BMS 180549, by different routes of administration. *Magn Reson Imaging* 1994;12:433-442
25. Taupitz M, Wagner S, Hamm B. Contrast media for magnetic resonance tomographic lymph node diagnosis (MR lymphography). *Radiologe* 1996;36:134-140
26. Vassallo P, Matei C, Heston WD, McLachlan SJ, Koutcher JA, Castellino RA. Characterization of reactive versus tumor-bearing lymph nodes with interstitial magnetic resonance lymphography in an animal model. *Invest Radiol* 1995;30:706-711
27. Weissleder R, Heautot JF, Schaffer BK, Nossiff N, Papisov MI, Bogdanov A Jr, et al. MR lymphography: study of a high-efficiency lymphotropic agent. *Radiology* 1994;191:225-230
28. Weissleder R, Elizondo G, Wittenberg J, Rabito CA, Bengele HH, Josephson L. Ultrasmall superparamagnetic iron oxide: characterization of a new class of contrast agents for MR imaging. *Radiology* 1990;175:489-493
29. Suga K, Yuan Y, Ogasawara N, Okada M, Matsunaga N. Localization of breast sentinel lymph nodes by MR lymphography with a conventional gadolinium contrast agent. Preliminary observations in dogs and humans. *Acta Radiol* 2003;44:35-42
30. Ruehm SG, Schroeder T, Debatin JF. Interstitial MR lymphography with gadoterate meglumine: initial experience in humans. *Radiology* 2001;220:816-821
31. Dimakakos E, Koureas A, Skiadas V, Kostapanagioutou G, Katsenis K, Arkadopoulou N, et al. Interstitial magnetic resonance lymphography with gadobutrol in rabbits and an initial experience in humans. *Lymphology* 2006;39:164-170
32. Trubetsky VS, Cannillo JA, Milshtein A, Wolf GL, Torchilin VP. Controlled delivery of Gd-containing liposomes to lymph nodes: surface modification may enhance MRI contrast properties. *Magn Reson Imaging* 1995;13:31-37
33. Harika L, Weissleder R, Poss K, Papisov MI. Macromolecular intravenous contrast agent for MR lymphography: characterization and efficacy studies. *Radiology* 1996;198:365-370
34. Kobayashi H, Kawamoto S, Star RA, Waldmann TA, Tagaya Y, Brechbiel MW. Micro-magnetic resonance lymphangiography in mice using a novel dendrimer-based magnetic resonance imaging contrast agent. *Cancer Res* 2003;63:271-276
35. Kobayashi H, Kawamoto S, Sakai Y, Choyke PL, Star RA, Brechbiel MW, et al. Lymphatic drainage imaging of breast cancer in mice by micro-magnetic resonance lymphangiography using a nano-size paramagnetic contrast agent. *J Natl Cancer Inst* 2004;96:703-708
36. Misselwitz B, Schmitt-Willich H, Michaelis M, Oellinger JJ. Interstitial magnetic resonance lymphography using a polymeric t1 contrast agent: initial experience with Gadomer-17. *Invest Radiol* 2002;37:146-151
37. Desser TS, Rubin DL, Muller H, McIntire GL, Bacon ER, Hollister KR. Interstitial MR and CT lymphography with Gd-dTPA-co-alpha, omega-diaminoPEG(1450) and Gd-dTPA-co-1,6-diaminohexane polymers: preliminary experience. *Acad Radiol* 1999;6:112-118
38. Herborn CU, Vogt FM, Lauenstein TC, Goyen M, Dirsch O, Corot C, et al. Assessment of normal, inflammatory, and tumor-bearing lymph nodes with contrast-enhanced interstitial magnetic resonance lymphography: preliminary results in rabbits. *J Magn Reson Imaging* 2003;18:328-335
39. Herborn CU, Lauenstein TC, Vogt FM, Lauffer RB, Debatin JF, Ruehm SG. Interstitial MR lymphography with MS-325: characterization of normal and tumor-invaded lymph nodes in a rabbit model. *AJR Am J Roentgenol* 2002;179:1567-1572
40. Choi SH, Han MH, Moon WK, Son KR, Won JK, Kim JH, et al. Cervical lymph node metastases: MR imaging of gadofluorine M and monocrySTALLINE iron oxide nanoparticle-47 in a rabbit model of head and neck cancer. *Radiology* 2006;241:753-762
41. Cha JH, Moon WK, Cheon JE, Koh YH, Lee EH, Park SS, et al. Differentiation of hyperplastic from metastatic lymph nodes using a lymph node specific MR contrast agent gadofluorine M. *J Korean Radiol Soc* 2006;55:183-189 [Korean]
42. Harisinghani MG, Barentsz J, Hahn PF, Deserno WM, Tabatabaei S, van de Kaa CH, et al. Noninvasive detection of clinically occult lymph-node metastases in prostate cancer. *N Engl J Med* 2003;348:2491-2499
43. Choi SH, Moon WK, Hong JH, Son KR, Cho N, Kwon BJ, et al. Lymph node metastasis: ultrasmall superparamagnetic iron oxide-enhanced MR imaging versus PET/CT in a rabbit model. *Radiology* 2007;242:137-143
44. Weissleder R, Elizondo G, Wittenberg J, Lee AS, Josephson L, Brady TJ. Ultrasmall superparamagnetic iron oxide: an intravenous contrast agent for assessing lymph nodes with MR imaging. *Radiology* 1990;175:494-498
45. Mühler A, Zhang X, Wang H, Lawaczek R, Weinmann HJ. Investigation of mechanisms influencing the accumulation of ultrasmall superparamagnetic iron oxide particles in lymph nodes. *Invest Radiol* 1995;30:98-103
46. Bush CH, Mladinich CR, Montgomery WJ. Evaluation of an ultrasmall superparamagnetic iron oxide in MRI in a bone tumor model in rabbits. *J Magn Reson Imaging* 1997;7:579-584

47. Rogers JM, Jung CW, Lewis J, Groman EV. Use of USPIO-induced magnetic susceptibility artifacts to identify sentinel lymph nodes and lymphatic drainage patterns. I. Dependence of artifact size with subcutaneous Combidex dose in rats. *Magn Reson Imaging* 1998;16:917-923
48. Bellin MF, Lebleu L, Meric JB. Evaluation of retroperitoneal and pelvic lymph node metastases with MRI and MR lymphangiography. *Abdom Imaging* 2003;28:155-163
49. Harisinghani MG, Dixon WT, Saksena MA, Brachtel E, Blezek DJ, Dhawale PJ, et al. MR lymphangiography: imaging strategies to optimize the imaging of lymph nodes with ferumoxtran-10. *Radiographics* 2004;24:867-878
50. Safety Data from Study 38804-10: A phase III safety and efficacy study of combidex as a magnetic resonance imaging agent for the evaluation of lymph node disease, AMAG. Pharmaceuticals, Inc., Boston, MA, USA
51. Islam T, Harisinghani MG. Overview of nanoparticle use in cancer imaging. *Cancer Biomark* 2009;5:61-67
52. Will O, Purkayastha S, Chan C, Athanasiou T, Darzi AW, Gedroyc W, et al. Diagnostic precision of nanoparticle-enhanced MRI for lymph-node metastases: a meta-analysis. *Lancet Oncol* 2006;7:52-60
53. Anzai Y, Piccoli CW, Outwater EK, Stanford W, Bluemke DA, Nurenberg P, et al. Evaluation of neck and body metastases to nodes with ferumoxtran 10-enhanced MR imaging: phase III safety and efficacy study. *Radiology* 2003;228:777-788
54. Saksena M, Harisinghani M, Hahn P, Kim J, Saokar A, King B, et al. Comparison of lymphotropic nanoparticle-enhanced MRI sequences in patients with various primary cancers. *AJR Am J Roentgenol* 2006;187:W582-W588
55. Narayanan P, Iyngkaran T, Sohaib SA, Reznick RH, Rockall AG. Pearls and pitfalls of MR lymphography in gynecologic malignancy. *Radiographics* 2009;29:1057-1069
56. Kimura K, Tanigawa N, Matsuki M, Nohara T, Iwamoto M, Sumiyoshi K, et al. High-resolution MR lymphography using ultrasmall superparamagnetic iron oxide (USPIO) in the evaluation of axillary lymph nodes in patients with early stage breast cancer: preliminary results. *Breast Cancer* 2009 [Epub ahead of print]
57. Heesakkers RA, Fütterer JJ, Hövels AM, van den Bosch HC, Scheenen TW, Hoogeveen YL, et al. Prostate cancer evaluated with ferumoxtran-10-enhanced T2\*-weighted MR Imaging at 1.5 and 3.0 T: early experience. *Radiology* 2006;239:481-487
58. Choi SH, Kim KH, Moon WK, Kim HC, Cha JH, Paik JH, et al. Comparison of lymph node metastases assessment with the use of USPIO-enhanced MR imaging at 1.5 T versus 3.0 T in a rabbit model. *J Magn Reson Imaging* 2010;31:134-141
59. Lahaye MJ, Engelen SM, Kessels AG, de Bruïne AP, von Meyenfeldt MF, van Engelshoven JM, et al. USPIO-enhanced MR imaging for nodal staging in patients with primary rectal cancer: predictive criteria. *Radiology* 2008;246:804-811
60. Lee AS, Weissleder R, Brady TJ, Wittenberg J. Lymph nodes: microstructural anatomy at MR imaging. *Radiology* 1991;178:519-522
61. Koh DM, Brown G, Temple L, Raja A, Toomey P, Bett N, et al. Rectal cancer: mesorectal lymph nodes at MR imaging with USPIO versus histopathologic findings--initial observations. *Radiology* 2004;231:91-99
62. Anzai Y, Prince MR. Iron oxide-enhanced MR lymphography: the evaluation of cervical lymph node metastases in head and neck cancer. *J Magn Reson Imaging* 1997;7:75-81
63. Anzai Y, Blackwell KE, Hirschowitz SL, Rogers JW, Sato Y, Yuh WT, et al. Initial clinical experience with dextran-coated superparamagnetic iron oxide for detection of lymph node metastases in patients with head and neck cancer. *Radiology* 1994;192:709-715
64. Bellin MF, Roy C, Kinkel K, Thoumas D, Zaim S, Vanel D, et al. Lymph node metastases: safety and effectiveness of MR imaging with ultrasmall superparamagnetic iron oxide particles--initial clinical experience. *Radiology* 1998;207:799-808
65. Sigal R, Vogl T, Casselman J, Moulin G, Veillon F, Hermans R, et al. Lymph node metastases from head and neck squamous cell carcinoma: MR imaging with ultrasmall superparamagnetic iron oxide particles (Sinerem MR) -- results of a phase-III multicenter clinical trial. *Eur Radiol* 2002;12:1104-1113
66. Stets C, Brandt S, Wallis F, Buchmann J, Gilbert FJ, Heywang-Köbrunner SH. Axillary lymph node metastases: a statistical analysis of various parameters in MRI with USPIO. *J Magn Reson Imaging* 2002;16:60-68
67. Mack MG, Balzer JO, Straub R, Eichler K, Vogl TJ. Superparamagnetic iron oxide-enhanced MR imaging of head and neck lymph nodes. *Radiology* 2002;222:239-244
68. Deserno WM, Harisinghani MG, Taupitz M, Jager GJ, Witjes JA, Mulders PF, et al. Urinary bladder cancer: preoperative nodal staging with ferumoxtran-10-enhanced MR imaging. *Radiology* 2004;233:449-456
69. Rockall AG, Sohaib SA, Harisinghani MG, Babar SA, Singh N, Jeyarajah AR, et al. Diagnostic performance of nanoparticle-enhanced magnetic resonance imaging in the diagnosis of lymph node metastases in patients with endometrial and cervical cancer. *J Clin Oncol* 2005;23:2813-2821
70. Stadnik TW, Everaert H, Makkat S, Sacré R, Lamote J, Bourgain C. Breast imaging. Preoperative breast cancer staging: comparison of USPIO-enhanced MR imaging and 18F-fluorodeoxyglucose (FDC) positron emission tomography (PET) imaging for axillary lymph node staging--initial findings. *Eur Radiol* 2006;16:2153-2160
71. Memarsadeghi M, Riedl CC, Kaneider A, Galid A, Rudas M, Matzek W, et al. Axillary lymph node metastases in patients with breast carcinomas: assessment with nonenhanced versus uspio-enhanced MR imaging. *Radiology* 2006;241:367-377
72. Heesakkers RA, Hövels AM, Jager GJ, van den Bosch HC, Witjes JA, Raat HP, et al. MRI with a lymph-node-specific contrast agent as an alternative to CT scan and lymph-node dissection in patients with prostate cancer: a prospective multicohort study. *Lancet Oncol* 2008;9:850-856
73. Fischbein NJ, Noworolski SM, Henry RG, Kaplan MJ, Dillon WP, Nelson SJ. Assessment of metastatic cervical adenopathy using dynamic contrast-enhanced MR imaging. *AJNR Am J Neuroradiol* 2003;24:301-311
74. Lee KC, Moon WK, Chung JW, Choi SH, Cho N, Cha JH, et al. Assessment of lymph node metastases by contrast-enhanced MR imaging in a head and neck cancer model. *Korean J Radiol* 2007;8:9-14
75. Murray AD, Staff RT, Redpath TW, Gilbert FJ, Ah-See AK, Brookes JA, et al. Dynamic contrast enhanced MRI of the axilla in women with breast cancer: comparison with pathology of excised nodes. *Br J Radiol* 2002;75:220-228
76. Luciani A, Dao TH, Lapeyre M, Schwarzinger M, Debaecque C, Lantieri L, et al. Simultaneous bilateral breast and high-resolution axillary MRI of patients with breast cancer: preliminary results. *AJR Am J Roentgenol* 2004;182:1059-1067